

Thermal reaction of iron with a Si(111) vicinal surface: Surface ordering and growth of CsCl-type iron silicide

A. Wawro,^{1,2*} S. Suto,³ R. Czajka,^{1,4} and A. Kasuya¹¹Center for Interdisciplinary Research, Tohoku University, Sendai 980–8578, Japan²Institute of Physics, Polish Academy of Sciences, Al. Lotników 32/46, 02–668 Warszawa, Poland³Department of Physics, Graduate School of Science, Tohoku University, Sendai 980–8578, Japan⁴Faculty of Technical Physics, Poznań University of Technology, ul. Niezawska 13A, 60–965 Poznań, Poland

(Received 23 September 2002; revised manuscript received 2 January 2003; published 5 May 2003)

The structural evolution of a vicinal silicon surface, developing upon low coverage deposition of Fe [0.33 and 2 monolayers (ML)], has been carefully studied as a function of annealing temperature by means of scanning tunneling microscopy. The reaction between the deposited material and the substrate, which occurs at room temperature, leads to surface amorphization. Successive annealing induces substantial changes of the surface structure. The onset of 2×2 reconstruction expansion of the Si surface, covered with 0.33 ML Fe, is observed after annealing at 400 °C. Complete reconstruction of the whole surface is found at the same temperature for a coverage of 2 ML. Upon annealing at 700 °C three-dimensional iron silicide islands grow epitaxially on the Si substrate. Their size, shape, and location depend on the amount of the deposited material. For 0.33 ML coverage elongated crystallites are distributed randomly on the vicinal substrate surface. Larger crystallites, grown upon deposition of 2 ML of Fe, take the shape of truncated pyramids and show a tendency to nucleate along vicinal surface terrace edges, forming a self-organized array of nanometer size dots. For both Fe coverages studied they are found to grow in a CsCl-type structure, containing an increasing amount of vacancies with increasing crystallite size. The electronic properties of iron silicide surface are probed with a spatial atomic resolution by means of tunneling spectroscopy. The interface between iron silicide crystallite and silicon substrate displays features characteristic of Schottky barriers.

DOI: 10.1103/PhysRevB.67.195401

PACS number(s): 68.35.–p, 75.50.Bb, 68.37.Ef, 81.07.–b

I. INTRODUCTION

The thin film Fe-Si system is the most intensively studied transition metal silicide due to the complexity of the formed compounds and an increasing interest in practical applications.^{1–6} Among a number of existing iron silicide phases particular attention is paid to the semiconducting β -FeSi₂. This phase has a narrow band gap of 0.87 eV, which corresponds to the maximum transmission of the optical fibers. Therefore, β -FeSi₂ is expected to be a suitable material, compatible with Si technology, for optoelectronic devices such as light detectors or near infrared sources. However, due to the variety of existing compounds and the complexity of process kinetics, a reliable recipe for the demanded structure of iron silicide thin films has not been unambiguously described yet. The reported results strongly depend on the growth conditions, affected by the applied deposition methods: codeposition by molecular beam epitaxy (MBE),^{7–15} reactive deposition epitaxy (RDE),^{16–18} and solid phase epitaxy (SPE).^{16–30}

In accordance with the Fe-Si phase diagram four equilibrium bulk compounds are stable: ferromagnetic Fe₃Si crystallizing in the DO₃ structure, metallic simple cubic ϵ -FeSi, high-temperature metallic tetragonal α -FeSi₂, and low-temperature semiconducting orthorhombic β -FeSi₂. However in thin iron silicide films epitaxially grown on Si substrate, strains induced at the interface, a consequence of the lattice mismatch, may substantially modify their crystalline structure. The semiconducting β -FeSi₂ phase, due to its orthorhombic structure, does not match well with the Si

lattice. Therefore the multidomain growth mode on Si(111) (Refs. 21,31–34) usually takes place as a result of stress accommodation at the interface. This disadvantage makes the implementation of the β phase difficult for practical usage in electronic devices. Stable in the bulk, but strained as a thin film, ϵ -FeSi phase exhibits a perfect (2×2) reconstruction.^{10,21,35–37} Also a high-temperature α -FeSi₂ phase, grown in nonequilibrium conditions, has been detected at room temperature.^{7–9,22,25,29,38–42} Phases FeSi_(1+x), where $0 < x < 1$, which have no counterpart in the bulk, display a pseudomorphic epitaxially stabilized CsCl-type structure.^{7,8,13,22,25,28,43} Reduced lattice mismatch lowers the strain energy at the interface, which plays the role of a basic stabilizing factor. With an increasing number of statistically distributed vacancies in Fe atom sites the phase composition evolves towards a higher Si content, approaching 1:2 stoichiometry. A metallic γ -FeSi₂ phase with a CaF₂-type structure is a result of such evolution.^{7,9,20,21,23–25,28,31,44} Although this compound is expected to be unstable in the bulk, because of the high density of states at the Fermi level,⁴⁵ the presence of the substrate is a driving force, which stabilizes it on the Si(111) surface. This phase might exhibit a behavior typical of a Stoner ferromagnet.

Iron silicide phase transition upon annealing has been a subject of intense controversy. Such a process is very sensitive to kinetic factors such as slight variations in the stoichiometry of the initial deposit and the substrate quality, its crystalline orientation, growth, and annealing rates. The transition temperature depends on the film thickness because the driving forces, which stabilize epitaxial phases, are affected

by the interface structure. Ultrathin films of γ phase^{7,20} and CsCl-type phase^{8,17} seem to be stable even at high temperature. A direct transition to the β phase^{7-9,17,21,23,29} or ϵ phase^{7,15,36,46} as well as a double stage transition via the ϵ phase to β phase¹⁰ occur in the case of thicker films. Lately the existence of a new metastable phase $L2$ has also been found.¹⁵ Moreover a reversible phase transition between the DO_3 - and the CsCl-type structures has been discovered very recently.⁴⁷ A diagram of phases and surface reconstructions, developed under various conditions, is shown in Ref. 24.

The composition of the topmost atomic layer of thin iron silicide films is another contradictory issue. Generally the Si termination layer^{19,21,27,48-51} or Si enrichment of the surface area^{16,42,47} has been inferred. The proposed models^{25,27} of the surface structure suggest that the double Si termination layer with Fe atoms located in the third and fourth atomic layer beneath the surface is formed. However, some experimental works as well as theoretical considerations reveal that the topmost surface layer consists mainly of Fe atoms.^{23,51}

The investigation of the early stage formation of iron silicide is the aim of this paper. By means of scanning tunneling microscopy (STM) we thoroughly study with atomic resolution the reactions which occur on a Si vicinal surface upon low-coverage Fe deposition, activated by subsequent successive annealing. Attention is also paid to the influence of vicinal surface structure on surface diffusion and—as a consequence—the growth of iron silicide crystallites. The iron silicide surface is studied by scanning tunneling spectroscopy (STS) with lateral atomic resolution. Also the properties of the interface between iron silicide crystallite and silicon substrate are investigated by spectroscopic techniques.

II. EXPERIMENTAL

Iron deposition and STM (Omicron) measurements were performed at room temperature in an UHV system at base pressure in the low range of 10^{-10} Torr. Commercial n -type Si(111) wafers (Sb doped, ~ 1 Ohm cm), misoriented by 1.2° in the $[-1-12]$ direction were used as the sample substrates. They were cut in the shape of bars with dimensions 1×9 mm². In order to get a clean Si(111) 7×7 surface, the substrates were heated up to 700°C for several hours, flashed at 1250°C up to five times and cooled down at a rate lower than 1°C/s . Such a thermal treatment resulted in the high quality of the 7×7 reconstruction with a negligible amount of the defects and contamination on the surface. As a consequence of misorientation the substrate surface had a terrace-like structure 800 – 1000 Å in width, separated by edge steps about 20 Å in average height. The iron was sublimated onto substrate from a tungsten basket at a rate of 5 Å/min. The deposition rates and the thickness were monitored by a quartz crystal microbalance. The atomic density of 1 ML is assumed to correspond to 1.2×10^{15} atoms cm⁻² as an average value of the low index surfaces of bcc Fe. STM measurements were performed directly after iron deposition and after subsequent annealing for 10 min at 250 , 400 , and 700°C . Tungsten STM tips were electrochemically etched and cleaned by annealing in the vacuum system. In our setup

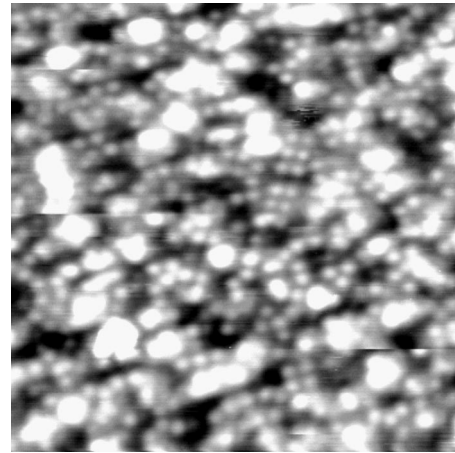


FIG. 1. Disordered Si(111) surface after deposition of 0.33 ML Fe. The size of the STM image is 200 Å \times 200 Å.

the sample is biased relatively to the tip—for positive voltage the empty states are imaged, whereas for negative bias—the filled ones are probed. All STM topographic images were recorded in the constant current mode.

III. RESULTS AND DISCUSSION

A. Reactions at low-temperature range

Deposition of 0.33 ML Fe on Si(111) substrate at room temperature substantially deteriorates the surface structure. Only small remaining fragments of 7×7 reconstruction are observable, as shown in Fig. 1. About 10 Å in diameter and one atomic monolayer in height clusters are randomly located on the disordered surface with well distinguished atoms, most probably Si. However, on the basis of merely topographic images it is not possible to distinguish unequivocally between disordered Fe and Si atoms. Most probably, as has been suggested earlier,²⁸ Fe atoms adsorb preferentially on three central adatoms of 7×7 unit cell and two or three Si atoms are expelled by the iron atom, which resides at the reaction site. Such observation is contrary to the case of the similar coverage of Au, deposited in the same conditions on the same type of silicon surface. Small Au clusters were located mainly in the center of both halves of a nondestroyed, very clearly distinguishable 7×7 unit mesh.⁵² Therefore comparing the results achieved upon Au and Fe deposition, it is reasonable to infer that the solid state reaction between sublimated Fe and the substrate occurs at room temperature.

Upon deposition of 2 ML of Fe, the tendency to form agglomerates a few nanometers in diameter is found. Due to a bigger amount of the deposited Fe, such clusters cover the whole surface without any visible remnants of 7×7 reconstruction, as seen for lower coverage. Their shapes are not regular and they are distributed uniformly on the whole surface.

Hitherto the reports on iron growth on a clean silicon surface at room temperature are somewhat contradictory. Epitaxial layer by layer growth of Fe, without any evidence of silicide formation was revealed in Refs. 18,19,26,53, and 54.

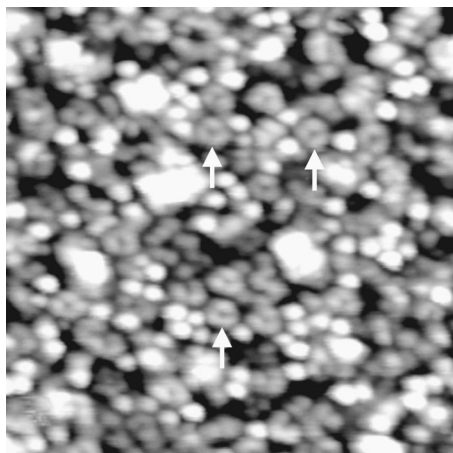


FIG. 2. STM topographic image ($200 \text{ \AA} \times 200 \text{ \AA}$) of 0.33 ML Fe after annealing at $250 \text{ }^\circ\text{C}$. Three atoms rings are in abundance on the surface (three exemplary rings are indicated by arrows).

However, in most experiments the reactivity of deposited Fe atoms with Si substrate was reported^{16,20,27,42,55–58} for lower coverages, even well below room temperature.²⁸ On the other hand, the growth of pure Fe on intermixed interface was observed^{2,34,35,57–59} in the case of higher coverages. Because in our experiment the thickness of deposited Fe did not exceed 2 ML, only amorphization of the surface took place upon deposition at room temperature.

The annealing at $250 \text{ }^\circ\text{C}$ initiates the ordering of the surface structure. In the sample with lower Fe coverage, three atoms rings are frequently encountered objects, as shown in Fig. 2. Each of these atoms is imaged in the same way at various biases, therefore they can be expected to be electronically equivalent. In this range of temperature a 1×1 surface reconstruction, inferred from diffraction techniques, has often been reported.^{12,27,28,42,60,61} However, the distance between ring member atoms, equal to 6.6 \AA , is much bigger than for Si-Si bonding in a bulk (3.86 \AA) rather fitting to that of the ϵ -FeSi phase.²¹ Because this phase is not observed at higher temperature, we suppose that formation of the rings is the initial stage of reconstruction of (CsCl) FeSi or γ -FeSi₂ phases, unequivocally identified after annealing at higher temperature. The distances between rings and their locations on the surface are random. The azimuthal planar orientation of all rings is the same, independent of the position on the surface, suggesting the influence of Si substrate symmetry on their formation process. These rings are the only ordered structures found on the surface. Between them, single atoms randomly located, occupy the remaining part of the surface. Also a certain amount of protrusions, one monolayer in height, consisting of few atoms, occasionally appears. No traces of long-range order are observed for this coverage.

For the coverage of 2 ML of Fe the onset of long-range ordering appears after annealing at $250 \text{ }^\circ\text{C}$. The surface is smoother than for the case of lower Fe coverage—the amplitude of cross-section profile does not exceed one monolayer distance. Nonregular in shape areas of close packed arrangement of atoms are distributed uniformly on the vicinal substrate terraces. The islands of ordered atoms cover approximately 20% of the whole surface. The comparison of the

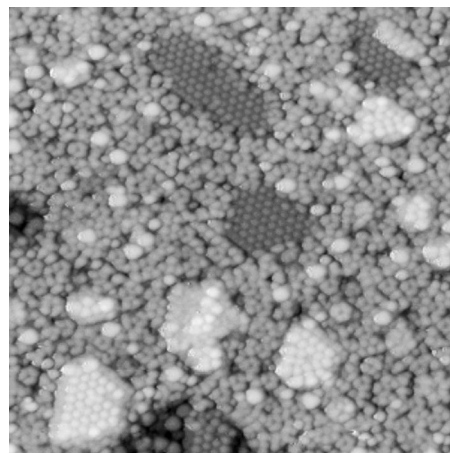


FIG. 3. Ordered islands with 2×2 alignment of atoms wrapped by a “sea” of unreconstructed surface with an abundance of three atoms rings, grown after annealing of 0.33 ML Fe at $400 \text{ }^\circ\text{C}$ (scan size: $375 \text{ \AA} \times 375 \text{ \AA}$).

observed structures leads to the conclusion that the process of surface ordering at this temperature is more advanced for higher Fe coverage.

B. Annealing at $400 \text{ }^\circ\text{C}$

The annealing of a sample with a coverage of 0.33 ML Fe at $400 \text{ }^\circ\text{C}$ results in further improvement of the surface structure. Three different areas of various arrangements of atoms are clearly distinguished at this stage of thermal treatment (Fig. 3). The islands of long-range ordered atoms, exhibiting hexagonal close packed structure, occupy the lowest and highest levels. Their shape is not regular and their position on the substrate terraces is random. The same azimuthal planar crystallographic orientation of all islands is evidence of the epitaxial growth, determined by the silicon substrate. The STM imaging of the topmost atoms is identical and does not depend on the applied bias, suggesting the same type of atoms. These well ordered islands, wrapped by the “sea” of the unreconstructed remaining part of the surface, cover about 10% of the observed area. The surface of the upper islands is 1.1 \AA above the level of the unreconstructed area, whereas that of the bottom one is 2 \AA below. The in-plane distance between nearest neighbor atoms, equal to 7.6 \AA , is compatible with reconstruction 2×2 both of γ -FeSi₂ (CaF₂) (Refs. 19,35) and (CsCl) FeSi (Ref. 7) structure grown in the [111] direction. The discernment between them merely on the basis of surface atom arrangement is not possible. Due to the vacancy-type structure of the γ phase, the distance between atomic layers in the [111] direction is twice as large as the CsCl-type structure, being equal to 3.1 and 1.6 \AA , respectively.^{7,10} The measured vertical distance between two surface levels of closely packed islands is quantized with 3.1 \AA , which favors the γ -FeSi₂ phase. However, further observations performed after annealing at higher temperature do not support γ phase existence, suggesting rather a CsCl-type structure of developing iron silicide. The presence of three member rings, appearing in the unreconstructed part of the substrate, the same as observed for this coverage upon

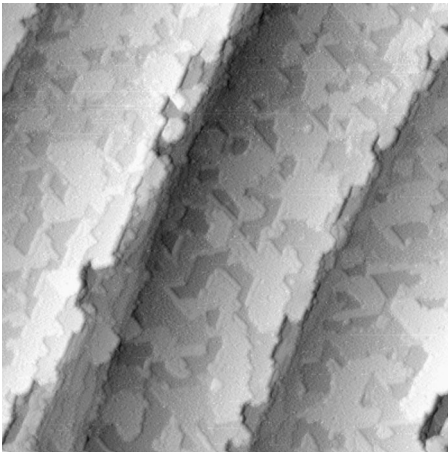


FIG. 4. Flat growth of iron silicide on Si vicinal surface. The STM image ($2000 \text{ \AA} \times 2000 \text{ \AA}$) was recorded after deposition of 2 ML annealed at 400°C .

annealing at 250°C , is another striking property. All previously found characteristic features: the distance of 6.6 \AA between ring constituting atoms, similar azimuthal orientation for all rings, and their random position on the surface are also encountered after thermal treatment at 400°C . The amount of rings is substantially larger than after annealing at 250°C . Our observation supports the earlier suggestions that the occurrence of such rings is a characteristic feature of low coverage, being a very initial formation stage of 2×2 reconstruction.

The reconstruction process at 400°C depends substantially on the iron coverage. For 2 ML of Fe the whole sample surface is uniformly terminated in the 2×2 alignment of atoms with the distance in plane between nearest neighbors equal to 7.6 \AA . Almost no vacancies are encountered, although linear defects such as borders of structural domain appear. The fluctuation of the surface height within the same terrace of the vicinal substrate does not exceed one monolayer. The very regular edges of atomically flat areas, oriented every 60° , are determined by the atomic rows (Fig. 4). The monoatomic terrace step height of 1.5 \AA corresponds to a value typical of the CsCl-type structure of iron silicide.

At higher resolutions two types of atoms in the topmost layer are easily recognized. Figure 5 shows the topographic image of the iron silicide surface recorded at negative bias voltage and two pairs of corrugation profiles of the same rows of atoms at the middle and the upper terminating layer, recorded at negative (-1.9 V) and positive ($+1.9 \text{ V}$) bias. The upper profiles correspond to empty states whereas the bottom ones correspond to occupied states. The surface atoms are imaged with different apparent heights under the same tunneling conditions. This feature is found to be the same for the middle and upper terminating layers. The observed difference indicates that the electronic structures of two types of atoms are not equivalent. Because various imaging is reproducibly achieved in the same scan, one may exclude the influence of the tip structure and associate an apparent topographic difference with a purely spectroscopic effect. Depending on the sign of the applied bias, the surface atoms are visible in the opposite way. It means that the at-

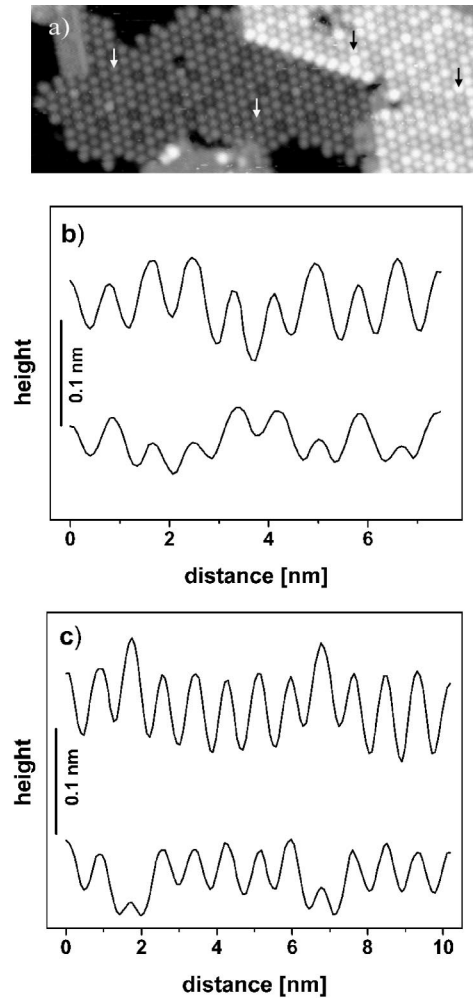


FIG. 5. (a) High resolution image ($225 \text{ \AA} \times 105 \text{ \AA}$) of 2×2 reconstructed surface after deposition of 2 ML Fe annealed at 400°C , recorded at a bias voltage of -1.9 V . Corrugation profiles of the same row of atoms taken on (b) upper terrace (between black arrows) and (c) bottom terrace (between white arrows). The upper profile in each set is recorded at $+1.9 \text{ V}$ and the bottom one at -1.9 V .

oms, which are imaged as “lower” for negative bias are slightly “higher” for positive bias. For further consideration this type of atom is assumed to be *A* type and the others are *B* type.

As mentioned earlier, the mean fluctuation of the surface height does not exceed one monolayer at the same terrace of the vicinal substrate. Therefore the surface of the sample is terminated by atomically flat terraces at three levels with quantized distance in the perpendicular direction typical of CsCl-type iron silicide structure, i.e., 1.5 \AA . The concentration of *A*-type atoms substantially depends on the level of atomic layer. At the lowest one all atoms are imaged in the same way. They are expected to be identical and of *B* type, as deduced from the surface profile consideration. In the middle layer a contribution of about 12% of *A*-type atoms is estimated. They are distributed rather uniformly without any tendency to agglomerate in clusters. The concentration of the *A*-type atoms is the highest in the topmost plane. A rough estimation reveals a similar contribution of *A*- and *B*-type

atoms. Although they are again distributed randomly on the surface, it frequently happens that two or more atoms of the same type (both *A* and *B*) neighbor each other. The position of the atoms of both types does not shift while changing the sign of the bias—they are only imaged with significantly different apparent heights. The absence of lateral shift suggests the lack of spatial separation of empty and occupied states.

At negative bias *A*-type atoms are imaged with lower apparent height by approximately 0.4 Å relatively to *B*-type atoms [bottom profiles in Figs. 5(b), 5(c)]. The positive bias inverts a way of imaging—the apparent height of *A*-type atoms is larger by 0.2 Å in comparison with *B*-type ones [upper profiles in Figs. 5(b), 5(c)]. The apparent height of atoms adjacent to atoms of different types seems to be unaffected by their neighborhood. For example in Fig. 5(c) *B*-type atoms adjacent to *A* type are of the same apparent height at both positive and negative bias as *B*-type atoms located in a uniform row. Also at the topmost terminating layer, where majority of atoms have neighbors of different type, their apparent height remains unaffected. This may be a proof of a strong localization of electronic states and weak interaction in the direction of the plane. Weak interaction between atoms may result from the relatively large separation distance of 7.6 Å between nearest neighbors.

Unequivocal chemical identification of the surface atoms, inferred from the STM measurements, is questionable. However, on the basis of available information, the conclusion on the nature of surface atoms, imaged by STM in different ways, might be drawn. A prevailing number of investigations reveals that the topmost layer of iron silicide is Si terminated.^{17,21,22,24,25,47,51,56} The presence of Si atoms decreases the surface energy.²¹ Several models of the double Si termination layer, with embedded Fe atoms on the third and fourth atomic planes underneath, have been proposed.^{25,27} Sparse contrary statements that Fe atoms might occupy the sites in the topmost layer or even iron silicide phase is Fe terminated,^{8,23,30,42} can also be found. Various imaging of the topmost atoms, while occupied states are probed, was reported in Ref. 19.

The Fe-Si bonding has a homopolar nature, however, in the FeSi(CsCl) phase the transfer of approximately 0.5 electronic charge per unit cell to *d* orbitals of Fe leads to a partial ionic character of this material.⁷ Such a charge transfer enhances the stability of CsCl-type phase. Therefore taking into account the abovementioned features, i.e., the Si termination layer and a charge transfer from Si to Fe as well as the better imaging of *sp* orbitals than *d* orbitals,⁴⁸ nonuniform distribution of *A*-type atoms exhibiting the trend of higher concentration on a higher terrace and three-dimensional growth of iron silicide crystallites upon annealing at 700 °C, discussed in the next section, the conclusion may be drawn that all surface atoms are Si, however, their STM imaging depends on their neighbors in the subsurface layer. If the adjacent atom is Fe, the topmost Si atom at negative bias is imaged as the “lower” one (described as the *A*-type atom). The neighborhood of the Si atom in the subsurface layer give rise to the “normal” imaging of the Si topmost atom (identified as a *B*-type atom). Therefore, we deduced that the nonuniform

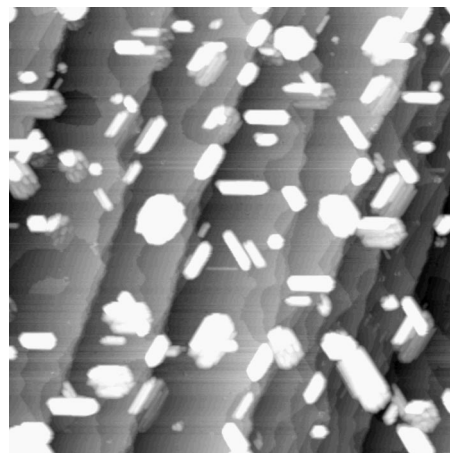


FIG. 6. Iron silicide nanocrystallites grown on the bare Si(111) 7×7 after annealing of 0.33 ML Fe at 700 °C. The scan size of the STM image is 500 Å×500 Å.

distribution of Fe atoms in the subsurface layer can be treated as an initial stage of islands formation of iron silicide on the bare Si(111) 7×7 surface, as observed after annealing at 700 °C.

C. Annealing at 700 °C

A further increase of annealing temperature drastically modifies the growth mode of iron silicide. Up to 400 °C iron silicide covers the entire surface uniformly, ordered in a various degree depending on the thickness of the deposited material. At 700 °C a strong tendency to three-dimensional island growth is evident.

Figure 6 shows the STM topographic image of 0.33 ML Fe after annealing at 700 °C. Iron silicide crystallites mostly take an elongated shape, but also nonregular islands are encountered. Between them there is a well reconstructed 7×7 surface of bare Si(111) with a very low amount of defects. Such growth, deduced from low energy electron diffraction (LEED) and Auger electron spectroscopy studies, has been reported earlier.²⁸ Evolution of a LEED pattern typical of 2×2 reconstruction towards that of 7×7 alignment, reported in Refs. 60,61, is associated with the dominating contribution of a bare Si surface in comparison with the area occupied by iron silicide crystallites, which still exhibit 2×2 reconstruction of the topmost layer (see the discussion in Sec. III E). The temperature of 700 °C is therefore high enough to activate a surface diffusion resulting in (i) agglomeration of Fe atoms, (ii) epitaxial growth of iron silicide crystallites on an Si surface, and (iii) complete reconstruction 7×7 of a bare silicon surface. One can expect that all deposited iron atoms are gathered in the volume of formed crystallites, because the annealing temperature is too low for re-evaporation from the sample surface. There is also clear evidence of the silicon surface etching process, which is necessary to supply atoms for the growth of iron silicide islands. On the terraces of vicinal silicon substrate numerous rounded terrace edges 3.2 Å in height, i.e., a double Si monolayer, are visible. They are not observed in such abundance and shape on the well reconstructed surface prior to Fe evaporation. The elongated

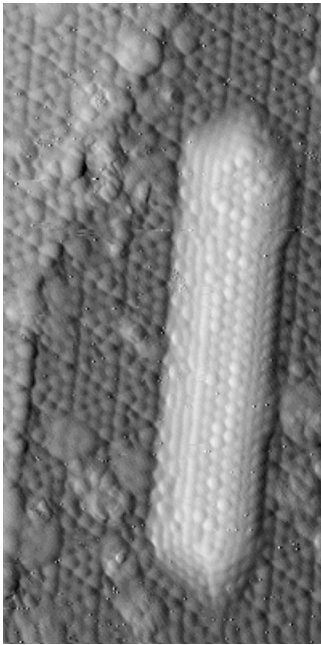


FIG. 7. STM derivative image ($200 \text{ \AA} \times 400 \text{ \AA}$) of single iron silicide nanocrystallite after annealing of 0.33 ML Fe at 700°C recorded at a bias of -2.27 V . Two types of surface atoms on the topmost layer and the facet are visible. Five atomic monolayers are very well distinguished on the bottom left-hand side facet.

crystallites of iron silicide are oriented along three directions, determined by the edges of the Si(111) 7×7 unit mesh. Their position with respect to the vicinal substrate terraces is random: they grow on the edges of vicinal surface terraces as well as in the center and even across the double Si monolayer step. Such abundance of the elongated crystallites might be evidence that they are an initial stage of iron silicide growth induced by annealing at 700°C . These structures take a rather uniform shape. Their length oscillates about 250 \AA . The topmost atomic layer displays a hexagonal close packed arrangement of atoms with the nearest neighbor distance equal to 7.6 \AA , which is typical of 2×2 reconstruction, also observed at lower temperatures, and favors CsCl-type or γ phase of iron silicide. However, on the basis of detailed cluster height analysis calibrated against the step height of Si substrate terrace, a quantization of about 1.5 \AA is found, which favors CsCl rather than a CaF_2 type of structure. The width of the elongated crystallites seems to be almost uniform and equal in most cases to three atomic rows on the crystallite surface.

The STM imaging of the topmost atoms is also bias dependent. For positive voltage, when the empty states of the sample are probed, no distinct difference between atoms is found. However at negative voltage some of them (described earlier as *B*-type atoms) appear brighter. Figure 7 shows an atomically resolved STM image of elongated crystallite of iron silicide, taken at a bias of -2.27 V . On the upper surface atoms with a larger apparent height by 0.6 \AA are very well distinguished. The variation of the apparent height of atoms when the bias voltage is changed indicates that they are not equivalent electronically. They exhibit a tendency to agglomerate in chains of several atoms. The same type of atoms is

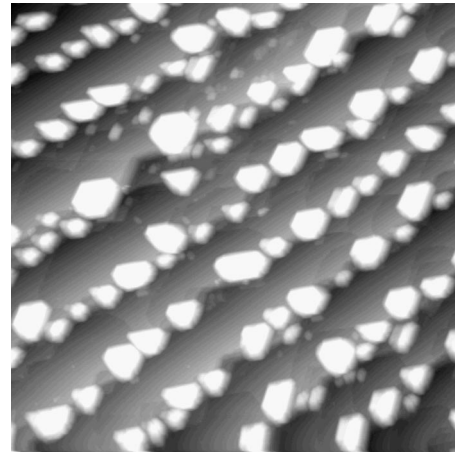


FIG. 8. STM image ($5000 \text{ \AA} \times 5000 \text{ \AA}$) of an iron silicide nanocrystallite array formed after annealing of 2 ML Fe at 700°C .

also found to be present on the facets of the crystallites. Excellent resolution of the image reveals that such a crystallite consist of five monolayers. Thus, in combination with its height of 7.9 \AA , there is unambiguous evidence that such a crystallite is of CsCl-type structure.

The crystallization process proceeds in a different way for thicker Fe coverage after annealing at 700°C . The growth of three-dimensional iron silicide islands takes place again (Fig. 8). However, in this case the truncated pyramids are the dominating shape of the protrusions, although a certain amount of elongated crystallites is also encountered. Similarly to the lower coverage, a very well reconstructed surface of silicon showing 7×7 structure appears between them. The location of clusters varies with increased coverage. For 2 ML of Fe they only decorate the upper edge of terraces of vicinal surface. None of them are located in the center of the terrace or across a step as in the case of lower coverages. This is probably due to the fact that for growth of such a structure upon deposition of a higher amount of Fe, the etching of the Si substrate is substantially more likely to form bigger crystallites and the edges of the terraces are energetically favored for such a solid state reaction. Such a mechanism of crystallization gives rise to the growth of self-organized iron silicide dots, which may find some practical application in nanoelectronics. The investigated phases of iron silicide are expected to be metallic and therefore might be a way to obtain a regular array of Schottky barriers. The periodicity of such structures in a direction perpendicular to the Si steps is determined by the width of vicinal surface terraces, resulting from the miscut of the silicon wafer, and in a direction parallel to the terrace edges it is determined by the Fe coverage.

The high-resolution image of a single iron silicide dot is shown in Fig. 9. The shape of a truncated pyramid positioned on the edge of the upper terrace of the vicinal surface with well defined facets of (100) and (111) type is very regular. The edges of the pyramid base are determined by the edges of the Si(111) unit mesh. The upper plane of the dot exhibits a 2×2 reconstruction—the same as observed earlier for the lower coverage after annealing at 400 and 700°C as well as

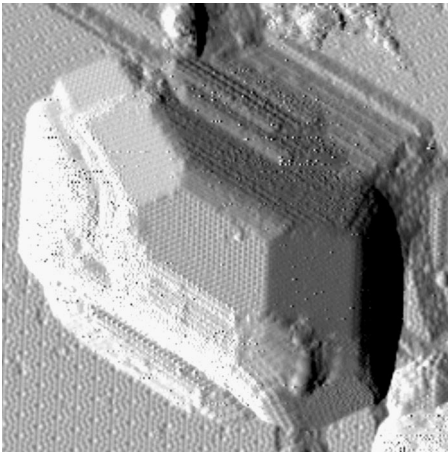


FIG. 9. High resolution STM derivative image ($625 \text{ \AA} \times 625 \text{ \AA}$) of a single iron silicide nanocrystallite grown after annealing of 2 ML of Fe at $700 \text{ }^\circ\text{C}$.

for 2 ML at $400 \text{ }^\circ\text{C}$. Therefore we can again consider CsCl or CaF_2 types of structures. On one of the side walls of the pyramid it is possible to distinguish its atomic structure. Taking into account the height of this cluster, equal to 68 \AA , and a number (more than 30) of atomic monolayers visible on the crystallite facet, the conclusion may be drawn that CsCl-type structure is expected rather than CaF_2 type. No difference in

atom imaging is observed both for positive and negative bias. Therefore one can infer that all atoms in the subsurface layer are of the same type, most probably Si. It seems that in this case the size of iron silicide crystallites is large enough to meet the conditions for the models^{25,27} of a double Si layer, which terminates the surface.

D. Spectroscopy

The various topographic imaging of the surface atoms of iron silicide crystallites grown at $700 \text{ }^\circ\text{C}$, discussed in the previous section, is clearly illustrated by the spectroscopic measurements. Figure 10 shows the topography image and two current maps (CITS), recorded at various biases, as well as I - V and dI/dV curves measured on two types of atoms of iron silicide dot and on the bare silicon surface for comparison. A part of the elongated crystallite is imaged as a bright vertically oriented area on the left hand side of the topography image [Fig. 10(a)]. A well reconstructed bare surface of Si substrate is visible in the background. In Fig. 10(b) the current image of the same area, recorded at a bias of 0.39 V , is shown. The atoms of silicon bare surface arranged in the 7×7 pattern are imaged as bright spots. The current image of iron silicide, visible as a dark stripe, reveals that the intensity of current flowing through the crystallite is much lower (for positive bias higher current corresponds to a brighter color). An entirely different CITS is achieved at a bias of -1.1 eV

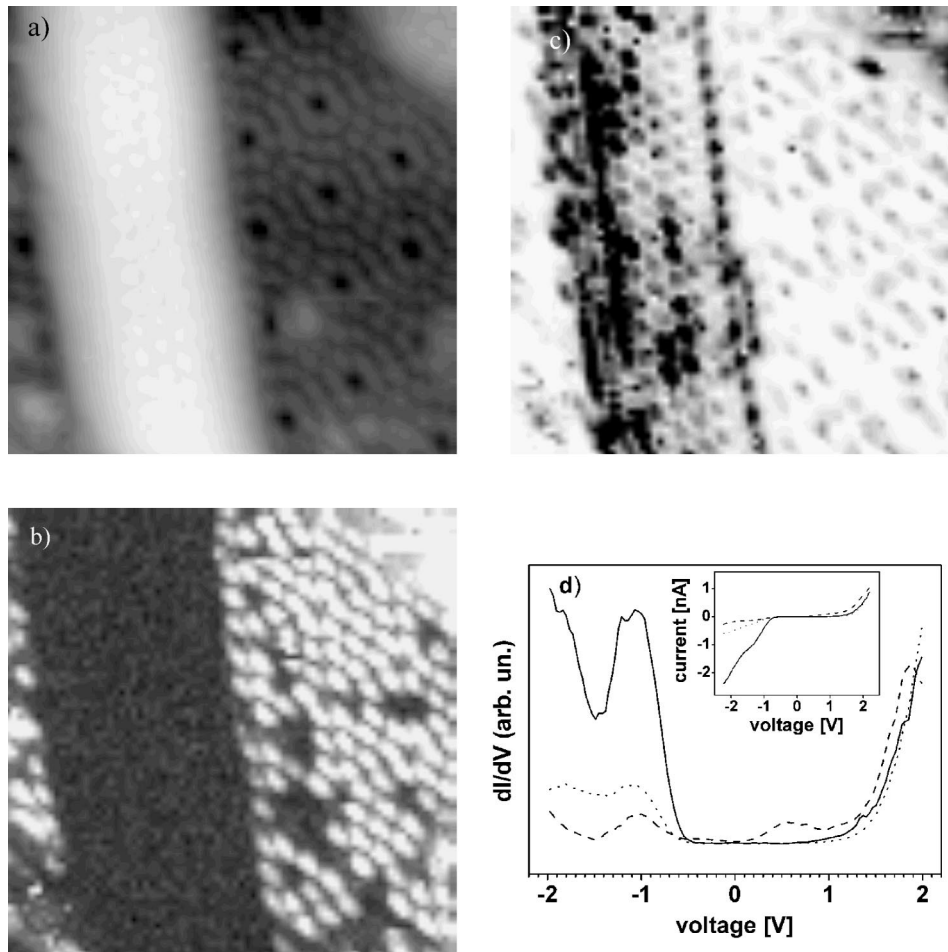


FIG. 10. (a) $150 \text{ \AA} \times 150 \text{ \AA}$ STM topography image recorded at $+2.27 \text{ V}$ of the iron silicide nanocrystallite (left side) grown on the bare Si(111) substrate (right side) after annealing of 0.33 ML Fe at $700 \text{ }^\circ\text{C}$. Current map (CITS) of the same area achieved at (b) $+0.39 \text{ V}$ and (c) -1.14 V . (d) Averaged dI/dV (in the insert I - V) curves recorded on a bare Si(111) surface (dashed line) and on the iron silicide nanocrystal topmost layer: A-type atoms (dot line) and B-type atoms (full line).

[Fig. 10(c)]. The surface of bare silicon is imaged rather uniformly; only weak contours of unit meshes are distinguishable. Individual atoms on the iron silicide crystallite surface are imaged in significantly different ways. These atoms, which are brighter in topography (Fig. 7), are observed in black in the current map (for negative bias higher current corresponds to darker color). About one fourth of the atoms which constitute the surface of the cluster exhibit such a property.

It is worth emphasizing that the observed difference in surface atom imaging is a purely spectroscopic effect. The stabilizing voltage while recording topography and spectroscopic curves was positive. Because all atoms show a similar corrugation for positive bias and the spatial distribution of the tunneling barrier height is expected to be uniform over the surface, because of small differences in the work functions for bulk Fe and Si, the parameters of the tunneling barrier are similar for both types of surface atoms. Thus various imaging at negative bias in the current map arises only from a different density of states of the two types of atoms.

Also darker imaging of the atoms along the bottom edge of the crystallite [Fig. 10(c)] reveals the higher current flowing through them. This phenomenon might be associated with the edge effect of the cluster, discussed below.

The I - V and dI/dV characteristics, typical of three different places, are shown in Fig. 10(d). Each curve has been averaged over at least ten runs obtained on various atoms of the same type. At positive bias above 1 V the shapes of all of them are very similar. This is associated with the fact that the topographic image of all atoms is identical in this range of the bias. The differences appear at low biases and when the occupied states are probed.

The dI/dV curve recorded on silicon substrate (dashed line) displays a relatively high density of surface states. Two well pronounced peaks above 0.3 eV and below -0.8 eV with maximums at 0.5 and -1.0 eV, correspond to conduction and valence bands, respectively. The dI/dV curves, recorded on iron silicide crystallite, differ from those for the silicon surface as well as from each other, depending on the type of atom. As for I - V curves the difference between them is negligible at positive bias. In the middle part, in the low bias range, they take a flat shape. Considerable differences in comparison to the silicon surface are recorded for occupied states. For both types of atoms on the iron silicide crystallite surface well pronounced peaks occur at -1.1 eV. They are slightly shifted towards lower energy compared to that of Si. The peak appearing for B -type atoms is much stronger than for A type.

This spectroscopic result supports the assumption that A -type atoms correspond to Si, which are adjacent to Fe in the subsurface layer, if the postulated shift of charge from silicon to iron atom^{7,26} is taken into consideration. The A -type atoms are in majority on the cluster's surface, which proves that in small iron silicide crystallites (only several monolayers in height), grown upon low-coverage deposition of Fe, the conditions to form double silicon layer termination^{25,27} are not met.

Spectroscopic data is also consistent if the studied system is considered in terms of Schottky barrier formation at the

interface between iron silicide crystallite and silicon substrate. The FeSi (CsCl) structure displays a metallic character, whereas the Si substrate is an n -type semiconductor. Therefore the depletion region and the band bending occurs in the semiconducting substrate in the vicinity of the interface. As a consequence an additional potential barrier is built-in at the junction. The appearance of such a barrier explains the lower current flowing through the iron silicide crystallite in comparison to bare silicon substrate for positive voltage [Fig. 10(b)]. For polarization, when the electrons tunnel from the tip through the cluster to the substrate, they encounter an additional barrier and the transmission probability is reduced. The opposite bias decreases the efficiency of the additional barrier and the tunneling probability increases. The evidence of Schottky barrier formation is well illustrated by dI/dV curves measured for both types of atoms of iron silicide crystallite. The extended flat region around zero bias, much larger than for bare silicon, reveals the occurrence of an additional potential barrier. Also the asymmetric shape of the I - V curve, particularly recorded for B -type atoms, resembles the diode-type character with the forward direction at the negative bias.

The existence of the Schottky barrier also explains the higher tunneling current flowing across edge atoms [Fig. 10(c)]. Near the edge of the interface the field intensity should be substantially larger than in the center of the crystallite. Thus the band bending is expected to be larger there and, as a consequence, the barrier width is expected to be smaller, which results in a higher intensity of the flowing current across that part of the contact.⁶²

E. Statistical analysis

In order to unequivocally determine the structure of iron silicide crystallites, formed upon deposition of 2 ML and subsequent annealing at 700 °C, detailed investigations of their height distribution have been carried out carefully. More than 80 randomly chosen dots were tested. The quantization of their height, calibrated as against the Si double atomic monolayer, is close to 1.5 Å, supporting the earlier presumptions that grown iron silicide is of CsCl-type structure. The histogram illustrating the distribution of crystallite height is shown in Fig. 11. Dots 7 nm in height dominate over much of the lower population of objects with smaller and larger heights. Such a finding leads to the conclusion that the process of iron silicide growth on vicinal Si substrates upon deposition of 2 ML and subsequent annealing at 700 °C has a tendency to form an array of very regularly shaped dots.

Another rough estimation method of cluster composition relies on the comparison of the volume of deposited Fe and the volume of crystallized iron silicide. Because the annealing temperature of 700 °C is too low for Fe reevaporation from the Si surface and between islands there is a bare well reconstructed Si(111) surface, it can be assumed that all the deposited material is contained in the iron silicide crystallites. For 0.33 ML Fe coverage the surface histogram analysis reveals that they occupy about 11% of the surface. Assuming that their mean height equals 8 Å, as obtained by

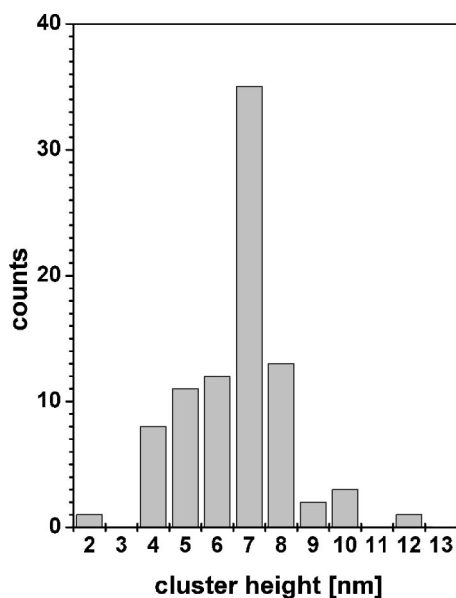


FIG. 11. Histogram of the iron silicide crystallite height grown after annealing of 2 ML Fe at 700 °C.

averaging over several tens of crystallites, their volume per area unit is approximately twice as large as the volume of deposited Fe, suggesting the composition 1:1 which corresponds to iron silicide growth in an CsCl-type structure with a negligible amount of vacancies in the Fe atomic site. A similar estimation was carried out for coverage of 2 ML of Fe. Taking into account the 13% coverage of sample surface and 66 Å as a mean height of iron silicide crystallites, one can deduce the presence of vacancies in the CsCl-type structure. The expectation that the structure of small crystallites is compact, whereas in bigger objects the vacancies may occur seems to be acceptable.

The structure estimation of iron silicide crystallites given above explains the observed composition of the topmost layer. In the case of small crystallites the fraction of surface atoms is relatively high. Therefore it is hard to expect that Fe atoms would be distributed very nonuniformly only in the inner part of the crystallite. As a consequence they should occupy a substantial number of sites in the subsurface layer, as observed for 0.33 ML Fe annealed at 700 °C. On the con-

trary, in bigger crystallites, formed upon annealing of 2 ML Fe at 700 °C, the amount of Si atoms is relatively higher and also the fraction of surface atoms is lower. Therefore it is more plausible that Fe atoms are distributed in the interior of iron silicide crystallite and on its surface there is only a double Si layer, as the mentioned models^{25,27} predicted.

IV. CONCLUSIONS

The evolution of the silicon surface structure, covered with iron, substantially depends on the annealing temperature and the amount of deposited material. The solid state reaction already takes place at room temperature. The successive increase of annealing temperature results in the improvement of the surface structure ordering. Up to 400 °C iron silicide has a tendency to grow in the two-dimensional mode. Surfaces with higher coverage (2 ML of Fe) are entirely reconstructed in a 2×2 pattern typical of CsCl-type structures. In the case of lower coverage the well reconstructed areas coexist with disordered parts of the surface. Qualitatively different growth modes develop after annealing at 700 °C. The intensive diffusion processes give rise to three-dimensional growth modes of monocrystalline iron silicide dots in a CsCl-type structure. Their shape and position on the vicinal surface depend on the coverage. For the lower one (0.33 ML of Fe) iron silicide crystallites take an elongated shape and their position on the substrate surface is random. A truncated pyramid shape prevails for higher coverages (2 ML of Fe). The vicinal structure of the surface determines the growth position of dots on the edge of the upper terraces, giving rise to a self-organized array pattern. The spectroscopic analysis shows that on the surface of smaller iron silicide dots, Fe atoms in the subsurface layer are present. Si enrichment of surface composition increases with the size of iron silicide crystallites leading to the double Si termination layer in the case of the biggest crystallites. The shape of spectroscopic curves suggests the existence of the Schottky barrier at the interface between the iron silicide dot and the semiconducting substrate.

ACKNOWLEDGMENTS

This work was partially supported by the State Committee for Scientific Research (Poland) under the project R-34.

*Corresponding author. Email: wawro@ifpan.edu.pl

¹C. R. M. Grovenor, *Microelectronic Materials* (Adam Hilger, Bristol, 1989).

²J. Derrien, J. Chevrier, V. Le Thanh, and J. E. Mahan, *Appl. Surf. Sci.* **56-58**, 382 (1992).

³M. C. Bost and J. E. Mahan, *J. Appl. Phys.* **58**, 2696 (1985).

⁴D. Leong, M. Harry, K. J. Reeson, and K. P. Homewood, *Nature (London)* **387**, 686 (1997).

⁵T. Suemasu, Y. Negishi, K. Takakura, and F. Hasegawa, *Jpn. J. Appl. Phys.* **39**, L1013 (2000).

⁶V. Bellani, G. Guizzetti, F. Marabelli, M. Patrini, S. Lagomarsino, and H. von Känel, *Solid State Commun.* **96**, 751 (1995).

⁷H. von Känel, K. A. Mäder, E. Müller, N. Onda, and H. Sirringhaus, *Phys. Rev. B* **45**, 13 807 (1992).

⁸H. Sirringhaus, N. Onda, E. Müller-Gubler, P. Müller, R. Stalder, and H. von Känel, *Phys. Rev. B* **47**, 10 567 (1993).

⁹N. Onda, J. Henz, E. Müller, K. A. Mäder, and H. von Känel, *Appl. Surf. Sci.* **56-58**, 421 (1992).

¹⁰N. Onda, H. Sirringhaus, E. Müller, and H. von Känel, *J. Cryst. Growth* **127**, 634 (1993).

¹¹C. Schwarz, N. Onda, S. Goncalves-Conto, H. Sirringhaus, H. von Känel, and R. E. Pixley, *J. Appl. Phys.* **76**, 7256 (1994).

¹²C. Pirri, M. H. Tuilier, P. Wetzel, S. Hong, D. Bolmont, G. Gewinner, R. Cortes, O. Heckmann, and H. von Känel, *Phys. Rev. B* **51**, 2302 (1995).

¹³K. L. Whiteaker, I. K. Robinson, C. Benson, D. M. Smilgies, N. Onda, and H. von Känel, *Phys. Rev. B* **51**, 9715 (1995).

¹⁴M. Fanciulli, C. Rosenblad, G. Weyer, A. Svane, N. E. Chris-

- tensen, and H. von Känel, *Phys. Rev. Lett.* **75**, 1642 (1995).
- ¹⁵M. Fanciulli, G. Weyer, A. Svane, N. E. Christensen, H. von Känel, E. Müller, N. Onda, L. Miglio, F. Tavazza, and M. Celino, *Phys. Rev. B* **59**, 3675 (1999).
 - ¹⁶J. M. Gallego, J. Alvarez, J. J. Hinarejos, E. G. Michel, and R. Miranda, *Surf. Sci.* **251-252**, 59 (1991).
 - ¹⁷N. Motta, A. Sgarlata, G. Gaggiotti, F. Patella, A. Balzarotti, and M. de Crescenzi, *Surf. Sci.* **284**, 257 (1993).
 - ¹⁸J. H. Oh, S. K. Lee, K. P. Han, K. S. An, and C. Y. Park, *Thin Solid Films* **341**, 160 (1999).
 - ¹⁹A. L. Vazquez de Parga, J. de la Figuera, C. Ocal, and R. Miranda, *Europhys. Lett.* **18**, 595 (1992).
 - ²⁰H. Moritz, B. Rösen, S. Popović, A. Rizzi, and H. Lüth, *J. Vac. Sci. Technol. B* **10**, 1704 (1992).
 - ²¹W. Raunau, H. Niehus, T. Schilling, and G. Comsa, *Surf. Sci.* **286**, 203 (1993).
 - ²²U. Kafader, M. H. Tuilier, C. Pirri, P. Wetzel, G. Gewinner, D. Blomont, O. Heckmann, D. Chandesris, and H. Magnan, *Europhys. Lett.* **22**, 529 (1993).
 - ²³W. Raunau, H. Niehus, and G. Comsa, *Surf. Sci. Lett.* **284**, L375 (1993).
 - ²⁴X. Wallart, J. P. Nys, and C. Tételin, *Phys. Rev. B* **49**, 5714 (1994).
 - ²⁵M. Sauvage-Simkin, N. Jedrecy, A. Waldhauer, and R. Pinchaux, *Physica B* **198**, 48 (1994).
 - ²⁶K. Rührschopf, D. Borgmann, and G. Wedler, *Thin Solid Films* **280**, 171 (1996).
 - ²⁷A. Mascaraque, J. Avila, C. Teodorescu, M. C. Asensio, and E. G. Michel, *Phys. Rev. B* **55**, R7315 (1997).
 - ²⁸W. Weiss, M. Kutschera, U. Starke, M. Mozaffari, K. Reshöft, U. Köhler, and K. Heinz, *Surf. Sci.* **377-379**, 861 (1997).
 - ²⁹N. Jedrecy, A. Waldhauer, M. Sauvage-Simkin, R. Pinchaux, and Y. Zheng, *Phys. Rev. B* **49**, 4725 (1994).
 - ³⁰J. J. Hinarejos, G. R. Castro, P. Segovia, J. Alvarez, E. G. Michel, R. Miranda, A. Rodriguez-Marco, D. Sánchez-Portal, E. Artacho, F. Ynduráin, S. H. Yang, P. Ordejón, and J. B. Adams, *Phys. Rev. B* **55**, R16065 (1997).
 - ³¹N. Cherief, C. D'Anterrosches, R. C. Cinti, T. A. Nguyen Tan, and J. Derrien, *Appl. Phys. Lett.* **55**, 1671 (1989).
 - ³²N. Cherief, R. Cinti, M. de Crescenzi, J. Derrien, T. A. Nguyen Tan, and J. Y. Veuillen, *Appl. Surf. Sci.* **41-42**, 241 (1989).
 - ³³A. Rizzi, H. Moritz, and H. Lüth, *J. Vac. Sci. Technol. A* **9**, 912 (1991).
 - ³⁴M. De Crescenzi, G. Gaggiotti, N. Motta, F. Patella, A. Balzarotti, and J. Derrien, *Phys. Rev. B* **42**, 5871 (1990).
 - ³⁵J. Chevrier, V. Le Thanh, S. Nitsche, and J. Derrien, *Appl. Surf. Sci.* **56-58**, 438 (1992).
 - ³⁶Le Thanh Vinh, J. Chevrier, and J. Derrien, *Phys. Rev. B* **46**, 15946 (1992).
 - ³⁷J. J. Hinarejos, P. Segovia, J. Alvarez, G. R. Castro, E. G. Michel, and R. Miranda, *Phys. Rev. B* **57**, 1414 (1998).
 - ³⁸X. W. Lin, M. Behar, J. Desimoni, H. Bernas, J. Washburn, and Z. Liliental-Weber, *Appl. Phys. Lett.* **63**, 105 (1993).
 - ³⁹J. Chevrier, P. Stocker, V. Le Thanh, J. M. Gay, and J. Derrien, *Europhys. Lett.* **22**, 449 (1993).
 - ⁴⁰F. Sirotti, M. De Santis, X. Jin, and G. Rossi, *Phys. Rev. B* **49**, 11134 (1994).
 - ⁴¹U. Kafader, C. Pirri, P. Wetzel, and G. Gewinner, *Appl. Surf. Sci.* **64**, 297 (1993).
 - ⁴²E. G. Michel, *Appl. Surf. Sci.* **117-118**, 294 (1997).
 - ⁴³M. Fanciulli, G. Weyer, J. Chevallier, H. von Känel, H. Deller, N. Onda, L. Miglio, F. Tavazza, and M. Celino, *Europhys. Lett.* **37**, 139 (1997).
 - ⁴⁴A. L. Vazquez de Parga, J. de la Figuera, C. Ocal, and R. Miranda, *Ultramicroscopy* **42-44**, 845 (1992).
 - ⁴⁵N. E. Christensen, *Phys. Rev. B* **42**, 7148 (1990).
 - ⁴⁶K. A. Mäder, H. von Känel, and A. Baldereschi, *Phys. Rev. B* **48**, 4364 (1993).
 - ⁴⁷U. Starke, J. Schardt, W. Weiss, W. Meier, C. Polop, P. L. de Andres, and K. Heinz, *Europhys. Lett.* **56**, 822 (2001).
 - ⁴⁸U. K. Köhler, J. E. Demuth, and R. J. Hamers, *Phys. Rev. Lett.* **60**, 2499 (1988).
 - ⁴⁹S. A. Chambers, S. B. Anderson, H. W. Chen, and J. H. Weaver, *Phys. Rev. B* **34**, 913 (1986).
 - ⁵⁰J. Alvarez, J. J. Hinarejos, E. G. Michel, J. M. Gallego, A. L. Vazquez de Parga, J. de la Figuera, C. Ocal, and R. Miranda, *Appl. Phys. Lett.* **59**, 99 (1991).
 - ⁵¹J. Junquera, R. Weht, and P. Ordejón, *Surf. Sci.* **482-485**, 625 (2001).
 - ⁵²A. Wawro (unpublished).
 - ⁵³T. Urano, T. Ogawa, T. Kanaji, and F. Fujimoto, *J. Vac. Sci. Technol. A* **5**, 2046 (1987).
 - ⁵⁴H. von Känel, R. Stalder, H. Sirringhaus, N. Onda, and J. Henz, *Appl. Surf. Sci.* **53**, 196 (1991).
 - ⁵⁵Y. Ufuktepe and M. Onellion, *Solid State Commun.* **76**, 191 (1990).
 - ⁵⁶J. Alvarez, A. L. Vazquez de Parga, J. J. Hinarejos, J. de la Figuera, E. G. Michel, C. Ocal, and R. Miranda, *Phys. Rev. B* **47**, 16048 (1993).
 - ⁵⁷M. Fanciulli, S. Degroote, G. Weyer, and G. Langouche, *Surf. Sci.* **377-379**, 529 (1997).
 - ⁵⁸R. Kläsages, C. Carbone, W. Eberhardt, C. Pampuch, O. Rader, T. Kachel, and W. Gudat, *Phys. Rev. B* **56**, 10801 (1997).
 - ⁵⁹B. Li, M. Ji, J. Wu, and C. Hsu, *J. Appl. Phys.* **68**, 1099 (1990).
 - ⁶⁰N. Minami, D. Makino, T. Matsumura, C. Egawa, T. Sato, K. Ota, and S. Ino, *Surf. Sci.* **514**, 211 (2002).
 - ⁶¹U. Starke, W. Weiss, M. Kutschera, R. Bandorf, and K. Heinz, *J. Appl. Phys.* **91**, 6154 (2002).
 - ⁶²D. L. Carroll, M. Wagner, M. Rühle, and D. A. Bonnell, *Phys. Rev. B* **55**, 9792 (1997).